Conservative Bias Linear Power Flow Approximations: Application to Unit Commitment

Paprapee Buason, Sidhant Misra
Los Alamos National Laboratory
Los Alamos, NM, USA
{buason, sidhant}@lanl.gov

Daniel K. Molzahn
School of Electrical and Computer Engineering
Georgia Institute of Technology
Atlanta, GA, USA
molzahn@gatech.edu

***Abstract*—The power flow equations are central to many problems in power system planning, analysis, and control. However, their inherent non-linearity and non-convexity present substantial challenges during problem-solving processes, especially for optimization problems. Accordingly, linear approximations are commonly employed to streamline computations, although this can often entail compromises in accuracy and feasibility. This paper proposes an approach termed *Conservative Bias Linear Approximations (CBLA)* for addressing these limitations. By minimizing approximation errors across a specified operating range while incorporating conservativeness (over- or under-estimating quantities of interest), CBLA strikes a balance between accuracy and tractability by maintaining linear constraints. By allowing users to design loss functions tailored to the specific approximated function, the bias approximation approach significantly enhances approximation accuracy. We illustrate the effectiveness of our proposed approach through several test cases, including its application to a unit commitment problem, where CBLA consistently achieves lower operating costs and improved feasibility compared to traditional linearization methods.**

***Index Terms*—Conservative bias linear approximation; power flow approximation; unit commitment.**

I. Introduction

The power flow equations play a central role in the operation and analysis of electric power systems. These equations are essential for evaluating the behavior of power networks, making them key to various optimization problems such as resilient infrastructure planning [1]–[3], AC unit commitment [4], [5], and bilevel problems [6], [7]. However, the nonlinearity of the power flow equations induces non-convexities in these problems that pose significant computational challenges.

To address these challenges, researchers have developed various linear approximations such as DC power flow [8], LinDistFlow [9], first-order Taylor expansions of the power flow equations, and other approximations [10]. These methods offer simplified representations of power flow, which improve the tractability of power systems optimization problems. However, these linearizations often depend on broad assumptions such as maintaining voltages near 1 per unit and keeping voltage angle differences small between neighboring buses, as in DC power flow. These assumptions may not be valid across all operating conditions, potentially resulting in inaccuracies in the approximations. Consequently, the solutions derived from these linearized models may not closely align with the actual optimal solutions in real-world scenarios. This trade-off between simplicity and accuracy necessitates careful consideration when applying these linearizations in practice.

In response to these challenges, various studies have explored *adaptive* power flow approximations tailored to specific systems and operating ranges to enhance approximation accuracy (e.g., optimization-based approaches in [11] and sample-based approaches in [12]–[14]); see [15]–[17] for recent survey papers on this concept. For sample-based approaches, samples of operating points computed by repeatedly solving the power flow equations at various points within an operating range (e.g., a specified range of power injections) are leveraged to compute the approximations. By capturing complex nonlinear relationships directly from these samples, the resulting linear approximations can be more accurate as they are formulated by minimizing deviations from the solutions provided by the AC power flow equations for a particular system and operating range of interest. These adaptive power flow linearizations spend computational effort to calculate the linearization coefficients in order to improve accuracy and tractability when applied in optimization problems. By trading up-front computational time for increased accuracy when applied, adaptive power flow approximations are particularly valuable in settings with both offline and online aspects where the linearization coefficients can be computed offline in advance of a real-time problem as well as settings where explicitly modeling power flow nonlinearities would lead to intractability, e.g., [1]–[7].

Extending the concept of sample-based adaptive power flow linearizations, the conservative linear approximation (CLA) approach in [12], [13] incorporates the concept of *conservativeness*. In other words, the CLAs are computed to minimize approximation errors with respect to the AC power flow equations while consistently over- or under-estimating quantities of interest over the set of drawn samples. The resulting approximations are particularly well suited for settings with an asymmetry in the implications of overestimating a quantity like voltage magnitude or current flow as opposed to underestimating that quantity. This is particularly relevant in power system optimization problems where feasibility is of paramount importance. For instance, when used in the bound on the magnitude of current flow through a line, a linearization that erroneously underestimates the amount of current flow risks

This work is supported by the advanced grid modeling (AGM) program of the Department of Energy, Office of Electricity and NSF award #2145564.

predicting feasibility when the constraint is actually violated with respect to the nonlinear AC power flow equations. This is a more problematic linearization error than an overestimate of the current flow for use in this constraint. Thus, conservative linearizations that avoid errors in a particular direction (i.e., avoid either overestimates or underestimates of some quantity) are valuable in many power system optimization contexts. However, maintaining conservativeness can sometimes lead to reduced accuracy.

In this paper, we introduce an approach to approximating power flow equations called *conservative bias linear approximation* (CBLA). The CBLA approach seeks to balance the trade-off between conservativeness and accuracy, particularly in scenarios where certain samples are challenging to approximate accurately. To construct CBLAs, the process shares similarities with CLAs by beginning with drawing samples from within the operational range. These samples form the basis of a regression problem, which is solved to compute an approximated function representing the power flow equations. However, unlike CLA, CBLA does not explicitly enforce conservativeness in its approximated function as a hard constraint. Instead, the CBLA approach introduces an error function that penalizes linearization errors for samples that violate conservativeness to enable more accurate approximations.

CBLA offers the advantage of flexibility in designing customized error functions that quantify the penalty for deviating from actual values. User-defined error functions enable the approach to be tailored to particular quantities of interest and system characteristics, thus computing a linearization specialized for a specific problem. This flexibility can be particularly beneficial in scenarios where some violations are permissible, such as in chance-constrained optimization problems.

This work extends our previous study presented in [18], where we introduced the CBLA approach for power flow linearization. In this journal version, we build upon that foundation by incorporating a unit commitment formulation [19] using CBLA, comparing it against other power flow linearization methods, and detailing a step-by-step process for solving the unit commitment problem.

In summary, the paper's main contributions are:

(*i*) A CBLA formulation that is tailored to the specific system and operating range, optimal with respect to an error metric, and strikes a balance between conservativeness and accuracy.

(*ii*) A discussion on choosing an error function for computing the CBLA.

(*iii*) Numerical tests of CBLAs for a variety of test cases.

(*iv*) An application and numerical results on proposed unit commitment problems comparing the CBLA approach with other power flow linearizations.

The remainder of this paper is organized as follows: Section II presents background material on power flow equations and sample-based conservative linear approximations. Section III introduces the proposed conservative bias linear approximation (CBLA) approach. Section IV describes the iterative method for solving the unit commitment problem using CBLA. Section V provides numerical results demonstrating the performance of the proposed method. Finally, Section VI concludes the paper and outlines directions for future research.

II. Background

In this section, we provide background information about the AC power flow equations and present the recently developed conservative linear approximations of these equations.

A. The Power Flow Equations

Consider a power system where a reference bus has the voltage angle set to 0. Let $V(\theta)$ denote the voltage magnitude (angle). Let $P(Q)$ denote the active (reactive) power injection. We use the subscript $(\cdot)_i$ to represent a quantity at bus i and the subscript $(\cdot)_{ik}$ to represent a quantity from or connecting bus i to k. Let $j = \sqrt{-1}$. The AC power flow equations at bus i are:

$$P_i = V_i^2 G_{ii} + \sum_{k \in \mathcal{B}_i} V_i V_k (G_{ik} \cos\theta_{ik} + B_{ik} \sin\theta_{ik}), \quad \text{(1a)}$$

$$Q_i = -V_i^2 B_{ii} + \sum_{k \in \mathcal{B}_i} V_i V_k (G_{ik} \sin\theta_{ik} - B_{ik} \cos\theta_{ik}), \quad \text{(1b)}$$

where $\theta_{ik} := \theta_i - \theta_k$, G and B are the real and imaginary parts of the system's admittance matrix, respectively, and $\mathcal{B}_i$ is the set of all neighboring buses to bus i, including bus i.

B. Conservative linear approximations

The nonlinearity of the power flow equations in (1) contributes to the complexity encountered in solving optimization problems. To address this challenge, we previously introduced a sample-based conservative linear approximation (CLA) approach aimed at either over- or under-estimating specified quantities of interest, such as the magnitudes of voltages and current flows (as illustrated in Fig. 1) [12]. Moreover, CLAs facilitate parallel computation by enabling concurrent computation of the CLA for each quantity of interest. The construction of a CLA entails sampling power injections across an operational range of interest, such as a range of loads and power generated by Distributed Energy Resources (DERs), followed by computing power flow solutions for each sample and solving a constrained-regression problem.

For instance, samples for load demands are acquired utilizing a predefined probability distribution $\mathbb{P}_{\mathcal{S}}$ over a specified operational range $\mathcal{S}$. This range could be defined as $\mathcal{S} = \{P_{L_d}^{\min} \le P_{L_d} \le P_{L_d}^{\max},\ Q_{L_d}^{\min} \le Q_{L_d} \le Q_{L_d}^{\max}$ for all $L_d \in \mathcal{N}_{\mathcal{D}}\}$, where $(\cdot)_{L_d}$ denotes the load demand, $\mathbb{P}_{\mathcal{S}}$ represents the uniform distribution, $\mathcal{N}_{\mathcal{D}}$ is the set of all buses with loads, and the superscripts max (min) indicate upper (lower) limits.

The utilization of CLAs allows for the customization of the approximation to fit a specific operating range and the targeted system. Additionally, the sample-based approach enables integrating the behavior of complicated devices like tap-changing transformers and smart inverters into the approximation, as discussed in our prior work [6]. In the realm of optimization, CLAs offer a crucial advantage: they enable the satisfaction of nonlinear constraints while enforcing only linear inequalities,

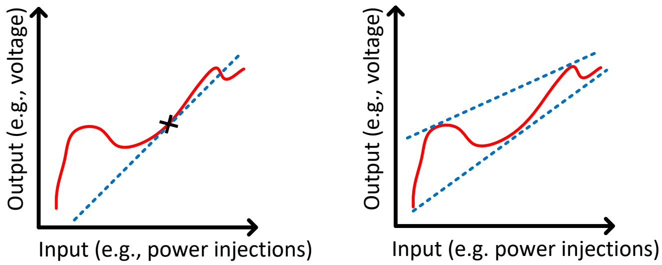

Fig. 1. An illustration showcasing a comparison between a conventional linear approximation (on the left) and CLAs (on the right). In this visual representation, the solid line signifies the nonlinear function under consideration. In the figure on the left, the dotted line represents a traditional first-order Taylor approximation centered at point $\times$, while in the figure on the right, the dotted line above (below) corresponds to an over- (under-)estimating approximation.

assuming the CLAs maintain conservativeness. Consequently, CLAs streamline optimization problems, rendering them suitable for commercial optimization solvers.

Consider a quantity of interest denoted as γ, which could represent variables such as the voltage magnitude at a specific bus or the magnitude of current flow along a particular line. In this context, bold quantities signify matrices and vectors. Let superscript T denote the transpose. An *overestimating* CLA can be expressed as follows:

$$a_0 + \boldsymbol{a}_1^T \begin{bmatrix} \boldsymbol{P} \\ \boldsymbol{Q} \end{bmatrix} \tag{2}$$

where a_0 is a scalar and $\boldsymbol{a}_1$ is a vector, both serving as decision variables in the regression problem later described in (4). This CLA is designed to ensure the following relationship for power injections $\boldsymbol{P}$ and $\boldsymbol{Q}$ within a specified range:

$$\gamma \leq a_0 + \boldsymbol{a}_1^T \begin{bmatrix} \boldsymbol{P} \\ \boldsymbol{Q} \end{bmatrix}. \tag{3}$$

Assuming that (3) is indeed satisfied, we can ensure that the constraint $\gamma \leq \gamma^{\max}$ is also satisfied by instead enforcing a linear constraint $a_0 + \boldsymbol{a}_1^T \begin{bmatrix} \boldsymbol{P} \\ \boldsymbol{Q} \end{bmatrix} \leq \gamma^{\max}$. This approach allows us to meet the upper bound requirement $\gamma^{\max}$ without introducing the implicit system of nonlinear AC power flow equations in (1). Importantly, by employing the CLA, we are able to satisfy the nonlinear equations while maintaining a linear formulation, thus enhancing computational tractability without sacrificing feasibility in the resulting solution.

To compute a CLA, we solve for the coefficients of the affine function of power injections in (2) in the following regression problem:

$$\min_{a_0,\ \boldsymbol{a}_1} \quad \frac{1}{M}\sum_{m=1}^{M} \mathcal{L}\left(\gamma_m - \left(a_0 + \boldsymbol{a}_1^T \begin{bmatrix} \boldsymbol{P}_m \\ \boldsymbol{Q}_m \end{bmatrix}\right)\right) \tag{4a}$$

$$\text{s.t.} \quad \gamma_m - \left(a_0 + \boldsymbol{a}_1^T \begin{bmatrix} \boldsymbol{P}_m \\ \boldsymbol{Q}_m \end{bmatrix}\right) \leq 0, \quad m = 1, \ldots, M. \tag{4b}$$

The subscript $(\,\cdot\,)_m$ denotes the m^{th} sample and M is the number of samples. The function $\mathcal{L}(\,\cdot\,)$ represents a loss function, such as the absolute value for ℓ_1 loss or the square for squared-ℓ_2 loss. In this paper, our focus is on quantities of interest denoted by γ, which correspond to the magnitudes of voltages (V) and current flows (I). The construction of underestimating CLAs follows a similar process as described in (4), with the key distinction being the reversal of the inequality direction in (4b).

The conservativeness of the CLA computed in (4) comes at the cost of reduced accuracy relative to the approximation corresponding to the unconstrained regression problem resulting from dropping (4a) from (4). To manage this tradeoff, the next section presents the main contribution of this paper, namely, a linear approximation technique that achieves a balance between conservativeness and accuracy. This approach involves biasing the linearization towards conservativeness, guided by a designated loss function.

III. Conservative Bias Linear Approximations

The CLA approach presented in Section II-B is consistently conservative within the set of drawn samples. However, in certain scenarios, the conservativeness property may lead to significant errors due to specific samples. In this paper, we present a sample-based *conservative bias linear approximation* (CBLA) approach that is adaptive, meaning it can be tailored to a specific system and operating range. The CBLA approach is designed to be optimal, minimizing a specific error metric while maintaining a *tendency to be conservative* to enhance accuracy. This means CBLA focuses on minimizing errors between the approximating function and the samples, allowing some samples to violate conservativeness at a specified cost.

A. Formulation

Let ϵ denote the mismatch between the approximated quantity and the actual quantity. The optimization problem to compute a CBLA is formulated as follows:

$$\min_{f(\epsilon_m(a_0, \boldsymbol{a}_1))} \quad \frac{1}{M}\sum_{m=1}^{M} f(\epsilon_m) \tag{5}$$

where

$$[\forall m = 1, \ldots, M]$$
$$\epsilon_m = \gamma_m - \left(a_0 + \boldsymbol{a}_1^T \begin{bmatrix} \boldsymbol{P}_m \\ \boldsymbol{Q}_m \end{bmatrix}\right), \tag{6}$$

and

$$f(\epsilon_m) = \begin{cases} g(\epsilon_m), & \text{if } \epsilon_m \leq 0 \\ h(\epsilon_m), & \text{otherwise.} \end{cases} \tag{7}$$

The optimization problem in (5) seeks to minimize the aggregated value of the error function $f(\,\cdot\,)$ defined in (7) over all samples by computing the coefficients a_0 and $\boldsymbol{a_1}$ in (6). This error function is contingent upon the error mismatch, denoted as ϵ in (6), between the estimated quantity and the actual quantity (γ). The error function is computed based on the error's sign for each sample. For *overestimation*, $h(\epsilon_m)$ is set high to impose a substantial cost for violation, while $g(\epsilon_m)$ is kept low for non-violations. Conversely, for *underestimation*, $h(\epsilon_m)$ is relatively low and $g(\epsilon_m)$ is high. For an alternative formulation of CBLA that incorporates a penalty term to influence the optimization behavior, see the appendix.

B. Error function

Choosing a suitable error function in the CBLA approach is an important consideration. The choice of error function depends on various factors, such as the specific system requirements, a quantity of interest, and the trade-off between accuracy and conservativeness. To better understand how the error function works, we compare the error function used in the CLA approach with that of the CBLA approach.

The CLA approach imposes conservativeness across the set of sampled data in the constraints. We can rewrite the regression problem described in (4), which utilizes the ℓ_1 loss function, as an optimization problem formulated in (5)–(7). In this formulation, the error function is defined as follows:

$$f(\epsilon_m) = \begin{cases} \epsilon_m, & \text{if } \epsilon_m \leq 0 \\ \infty, & \text{otherwise.} \end{cases} \tag{8}$$

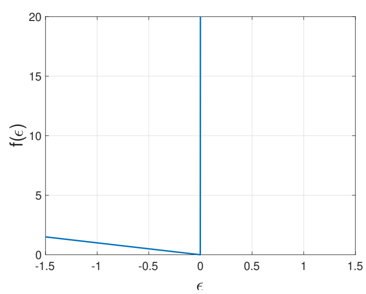

Fig. 2. An error function of the CLA where $g(\epsilon) = \epsilon$ and $h(\epsilon) = \infty$.

The error function in (8) (see Fig. 2) assigns an infinite cost to any violation of the overestimating requirement. This implies that for all samples drawn, no violation is permitted.

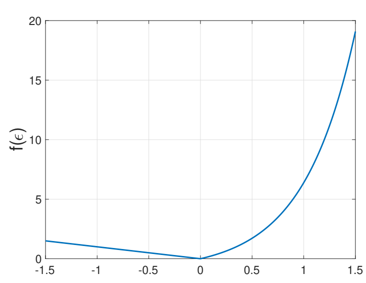

Fig. 3. An example of an error function where $g(\epsilon) = \epsilon$ and $h(\epsilon) = e^{2\epsilon} - 1$.

In contrast, our CBLA approach offers the flexibility to configure an error function that accommodates violations for specific samples, all while considering a predefined cost associated with these violations. This ability to tailor the error function empowers us to strike a balance between accuracy and the acceptable level of conservativeness for the specific system and operating range of interest. In Fig. 3, an example of an error function $f(\epsilon)$ for an overestimating CBLA is depicted. The function $f(\epsilon)$ exhibits a high value for $\epsilon > 0$, $f(\epsilon)$ maintains a relatively low value for $\epsilon < 0$, and $f(0)$ is zero, indicating an exact approximation.

In this setup, assigning a higher penalty for violations of conservativeness leads to more conservative approximations at the expense of some accuracy. Additionally, when the derivative of the function $h(\epsilon)$ increases, as shown in Fig. 3, the function tends to allow only small positive values of ϵ, because larger positive values result in exponentially higher penalties. Conversely, reducing the penalty cost tends to produce more accurate approximations but with less conservativeness.

When the error function is defined as a piecewise linear function (i.e., when both $g(\epsilon)$ and $h(\epsilon)$ are linear functions), the problem formulation to compute CBLAs in (5)–(7) can be framed as a linear program as follows:

$$\min_{a_0,\ \boldsymbol{a}_1} \quad \frac{1}{M} \sum_{m=1}^{M} z_m \tag{9a}$$

$$\text{s.t.} \quad [\forall m = 1, \ldots, M]$$

$$\epsilon_m = \gamma_m - \left(a_0 + \boldsymbol{a}_1^T \begin{bmatrix} \boldsymbol{P}_m \\ \boldsymbol{Q}_m \end{bmatrix} \right), \tag{9b}$$

$$z_m \geq k_1 \epsilon_m, \tag{9c}$$

$$z_m \geq k_2 \epsilon_m, \tag{9d}$$

where z is a slack variable, and k_1 and k_2 are the coefficients of the linear error functions, i.e., $g(\epsilon) = k_1 \epsilon$ and $h(\epsilon) = k_2 \epsilon$.

Nonlinear error functions transform the regression problem into a mixed-integer nonlinear program. This can be efficiently implemented using a user-defined function in Julia and solved with packages such as Optim, which offers a robust framework for constrained optimization problems [20].

IV. Unit Commitment

The unit commitment (UC) problem is an optimization problem in power system operations that aims to determine the optimal schedule of generating units over a specified time horizon, typically 24 hours. The primary goal is to minimize the total cost of operation while ensuring that the demand for electricity is met and the technical and operational constraints of the generation units and transmission network are satisfied.

The variability and uncertainty associated with loads, particularly when load shedding may be necessary, and generation introduce additional complexities that the unit commitment (UC) problem must address to ensure grid reliability and operational efficiency. As a mixed-integer optimization problem, the UC formulation involves binary variables to represent the on/off status of generators, along with continuous variables to model power output.

A. Computational procedure and parallelization potential

Solving the unit commitment problem using CBLA involves multiple computational steps, each contributing to accurately determining generator commitments and dispatch while leveraging efficient approximations of power flow equations. Given the complexity of unit commitment and the nonlinearity of AC power flow, CBLA serves as an effective method to construct computationally efficient linear approximations. The overall process consists of three key steps:

1) **CBLA computation**: Solve the CBLA formulation in (5) to approximate voltage and current over a range of operating conditions. This step requires generating samples within expected operating ranges and solving the CBLA optimization problem.
2) **Unit commitment optimization**: Using the CBLA approximations obtained in Step 1, solve the UC problem to determine generator statuses for each generator at each hour while ensuring operational constraints are satisfied.
3) **AC optimal power flow (AC OPF) evaluation**: Given the generator statuses from Step 2, solve the AC OPF that allows load shedding to determine the generation dispatch at each hour, ensuring feasibility under AC power flow constraints [21].

This computational framework allows parallel execution, particularly in Steps 1 and 3. In Step 1, solving CBLA involves two key computations that can be parallelized. First, the power flow solutions at each operating point can be computed independently. Second, the regression problem for the CBLA can be solved independently for each quantity, using the same set of samples across all regression problems. Similarly, in Step 3, since ramping constraints are not enforced and only minimum up- and down-time constraints are considered, the AC OPF computations at different time steps are independent once generator statuses are fixed, enabling parallel execution across time periods. Fig. 4 illustrates the full set of computational steps required to solve the unit commitment problem using the CBLA approach.

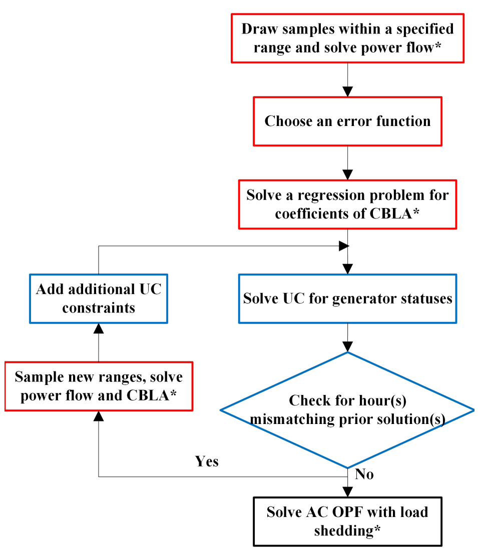

Fig. 4. A flowchart illustrating the computational process for solving the unit commitment (UC) problem using CBLA. Steps enclosed in red boxes correspond to CBLA, while steps enclosed in blue boxes relate to the UC problem. Steps marked with $*$ indicate parallelizable processes.

B. Optimization Problem Formulation

Let $u_{g,t}$ be a generator on/off status and $s_{g,t}$ $(r_{g,t})$ be a generator startup (shutdown) status for generator g at time t. The unit commitment problem with the DC power flow [22] is formulated as follows:

$$\min \sum_{t\in\mathcal{T}} \left(\sum_{g\in\mathcal{G}} c_g(P_{g,t}) + C_g^{\text{startup}} s_{g,t} + C_g^{\text{shutdown}} r_{g,t} \right) \tag{10a}$$

$$\text{s.t.} \sum_{g\in\mathcal{G}} P_{g,t} = D_t, \quad \forall t \in \mathcal{T}, \tag{10b}$$

$[\forall g \in \mathcal{G}]$

$$P_{g,t} \le P_g^{\max} u_{g,t},\ P_{g,t} \ge P_g^{\min} u_{g,t},\ \forall t \in \mathcal{T}, \tag{10c}$$

$$s_{g,t} - r_{g,t} = u_{g,t} - u_{g,t-1},\ \forall t \in \mathcal{T}, \tag{10d}$$

$$\sum_{\tau=t}^{t+T_g^{\text{up}}-1} u_{g,\tau} \ge T_g^{\text{up}} \Big(u_{g,t} - u_{g,t-1} \Big), \quad \forall t \in \{1,\dots,T-T_g^{\text{up}}\}, \tag{10e}$$

$$\sum_{\tau=t}^{t+T_g^{\text{down}}-1} (1-u_{g,\tau}) \ge T_g^{\text{down}} \Big(u_{g,t-1} - u_{g,t} \Big), \quad \forall t \in \{1,\dots,T-T_g^{\text{down}}\}, \tag{10f}$$

$$\theta_{i,t} - \theta_{k,t} = \frac{P_{ik,t}}{B_{ik}},\ \forall (i,k) \in \mathcal{L}, \forall t \in \mathcal{T}, \tag{10g}$$

$$-P_{ik}^{\max} \le P_{ik,t} \le P_{ik}^{\max},\ \forall (i,k) \in \mathcal{L}, \forall t \in \mathcal{T}, \tag{10h}$$

where $u_{g,0} = 0$ for all g, $c_g(P_{g,t})$ is a cost associated with generator g at time t (for example, $c_g(P_{g,t}) = c_{2g}P_{g,t}^2 + c_{1g}P_{g,t} + c_{0g}$ for a polynomial cost function), $\mathcal{G}$ is a set of all generators, $\mathcal{L}$ is a set of all lines, and $\mathcal{T}$ is a set of time in hours.

The optimization problem in (10) is referred to as the UC problem, which minimizes the total operating cost over a given time horizon. The objective function in (10a) comprises generation costs, startup costs, and shutdown costs.

The constraint (10b) ensures power balance at every time step, requiring total generation to match load demand, where (10c) enforces that the power output of each generator stays within its operational limits when the generator is online. The constraint (10d) models the relationship between the on/off status of generators and their startup/shutdown states. In this setup, we consider ramping constraints as part of the startup and shutdown constraints, ensuring that generation changes smoothly during transitions. The constraints (10e)–(10f) enforce minimum up-time and down-time requirements for generators, ensuring they remain online or offline for a specified duration after being switched on or off. The constraint (10g) represents the linearized DC power flow equations, relating power flows to voltage angle differences and line susceptance. Finally, (10h) ensures that power flow on each line does not exceed its thermal limits in either direction.

To extend this formulation and provide a baseline for comparison, the appendix presents a set of linear constraints based on the first-order Taylor approximation of voltage magnitudes and current flows.

C. Unit commitment using conservative bias linear approximations

The unit commitment problem formulated in the previous subsection enforces network feasibility using a DC power flow approximation. While computationally efficient, the DC power flow model does not explicitly incorporate voltage and current constraints. In this section, we introduce penalty terms and replace the DC power flow constraints in (10g)–(10h) with a CBLA, which provides a linearized yet conservative representation of these constraints.

Let $\mathcal{B}$ be a set of all buses. The CBLA enforces voltage magnitude limits at each bus using the following inequalities:

$$\underline{a}_{0,i,t} + \underline{\boldsymbol{a}}_{1,i,t}^T \begin{bmatrix} \boldsymbol{P_t} \\ \boldsymbol{Q_t} \end{bmatrix} \geq V_i^{\min} - v_{i,t}^{\min},\ \forall i \in \mathcal{B}, \forall t \in \mathcal{T}, \quad (11a)$$

$$\overline{a}_{0,i,t} + \overline{\boldsymbol{a}}_{1,i,t}^T \begin{bmatrix} \boldsymbol{P_t} \\ \boldsymbol{Q_t} \end{bmatrix} \leq V_i^{\max} + v_{i,t}^{\max},\ \forall i \in \mathcal{B}, \forall t \in \mathcal{T}, \quad (11b)$$

where $v_{i,t}^{\min}$ and $v_{i,t}^{\max}$ are nonnegative penalty variables that allow violation of the voltage approximations at bus i at time t. Here, $\boldsymbol{P}_t$ ($\boldsymbol{Q}_t$) denotes the vector of active (reactive) power injections at time t, while $V_i^{\min}$ and $V_i^{\max}$ are the lower and upper voltage magnitude limits at bus i. The coefficients $\underline{a}_{0,i}$ and $\underline{\boldsymbol{a}}_{1,i}$ correspond to the underestimating voltage approximation at bus i, and $\overline{a}_{0,i,t}$ and $\overline{\boldsymbol{a}}_{1,i,t}$ correspond to the overestimating voltage approximation.

Additionally, we enforce current flow limits in transmission lines through the following constraint:

$$\overline{b}_{0,ik,t} + \overline{\boldsymbol{b}}_{1,ik,t}^T \begin{bmatrix} \boldsymbol{P_t} \\ \boldsymbol{Q_t} \end{bmatrix} \leq I_{ik}^{\max} + z_{ik,t},\ \forall (i,k) \in \mathcal{L}, \forall t \in \mathcal{T}, \quad (12)$$

where $z_{ik,t}$ is a nonnegative penalty variable allowing violation of the current flow approximation on line (i,k) at time t, $I_{ik,t}^{\max}$ denotes the maximum allowable current on line (i,k), and $\overline{b}_{0,ik,t}$, $\overline{\boldsymbol{b}}_{1,ik,t}$ are coefficients for the overestimating current flow.

Let $F(\boldsymbol{P}_{g,t}, \boldsymbol{s}_{g,t}, \boldsymbol{r}_{g,t})$ denote the objective function in (10a). With the inclusion of penalty terms, the modified objective becomes:

$$F(\boldsymbol{P}, \boldsymbol{s}, \boldsymbol{r}) + \sum_{t \in \mathcal{T}} \left(\lambda \sum_{(i,k) \in \mathcal{L}} z_{ik,t} + \gamma \sum_{i \in \mathcal{B}} (v_{i,t}^{\max} + v_{i,t}^{\min}) \right), \quad (13)$$

where λ and γ are the penalty weights associated with violations of current and voltage magnitude constraints, respectively.

The CBLA method constructs linear constraints from coefficients derived at sampled operating points within a specified range. Before solving the UC problem, we can identify buses and lines that do not exhibit voltage or current violations in the sampled data; constraints for these elements remain inactive and can be excluded, reducing computational complexity without compromising feasibility.

By incorporating these constraints into the UC problem, CBLA ensures generation schedules remain feasible with respect to voltage and line flow limits while maintaining computational tractability. Unlike the standard DC power flow model, CBLA systematically accounts for these limits through conservative yet efficient linear approximations. Its sample-based nature also enables constraint screening, identifying likely binding constraints and allowing flexibility in selecting the error function depending on whether voltage or line flow limits are active.

To maintain the validity of CBLA-based constraints during the UC process, we adopt an iterative approach (Fig. 4). In each iteration, we solve the UC problem with the current CBLA, then check if the generation statuses and dispatch levels match those from a first-order Taylor-based method or previous CBLA iterations. We also verify whether power injections stay within the sampled region used to build the CBLA. If violations occur, we identify the affected time periods and buses or lines, draw new samples around the updated solution, recompute the CBLA, and resolve the UC problem. This process prevents accuracy degradation from extrapolation and cycling between inconsistent UC solutions.

This CBLA-based formulation further allows two practical enhancements. First, it offers flexibility in controlling conservativeness by adjusting a bias term when constructing the constraints, enabling the user to trade off between feasibility margin and conservatism. Second, it supports the inclusion of penalty terms that allow for controlled constraint violations, enhancing feasibility in cases where a strictly conservative formulation may be overly restrictive.

D. Combinatorial Growth of Valid Generator Statuses

In the unit commitment formulation, each generator's on/off status over time must satisfy minimum up and down time constraints (10e)–(10f), substantially reducing the number of admissible on/off sequences. Nevertheless, the feasible status space still grows exponentially with the number of time periods, making brute-force enumeration impractical.

To quantify this space, we implement an enumeration algorithm that counts binary vectors of length $|\mathcal{T}|$ satisfying a minimum run length $d = T^{\text{up}} = T^{\text{down}}$ for both states, allowing exceptions for an initial short off-run and final short runs. Due to these exceptions, a clean closed-form expression is difficult to derive. Instead, the number of valid vectors is characterized recursively: sequences are built by appending valid runs (of at least length d) to shorter valid sequences, naturally leading to a dynamic programming approach.

Let $f(|\mathcal{T}|, s, \ell)$ denote the number of valid binary sequences of length $|\mathcal{T}|$, ending in state $s \in \{0,1\}$ with a current run of length ℓ. The recurrence relation is:

$$f(|\mathcal{T}|, s, \ell) = \begin{cases} \sum_{k=d}^{\lfloor |\mathcal{T}|/2 \rfloor} f(|\mathcal{T}| - k, 1 - s, k), \text{ if } \ell = d, |\mathcal{T}| \geq d \\ f(|\mathcal{T}| - 1, s, \ell - 1), \text{ if } \ell > d \\ 1, \text{ if } |\mathcal{T}| = \ell \leq d, \text{ one of the exceptions holds} \\ 0, \text{ otherwise} \end{cases}$$

where the exceptions include:

- Initial 0's from position 1 with length less than d,
- Final 0's or 1's from position $|\mathcal{T}| - d + 2$ onward.

The total number of valid sequences is

$$F(|\mathcal{T}|) = \sum_{s \in \{0,1\}} \sum_{\ell=1}^{|\mathcal{T}|} f(|\mathcal{T}|, s, \ell).$$

For example, with $|\mathcal{T}| = 5$ and $d = 2$, applying the recurrence yields 13 valid sequences for a single generator. Therefore, for 6 generators, the total number of configurations is $(F(5))^6 = 13^6 =$ 4,826,809, demonstrating how the feasible status space grows rapidly even for modest systems. This growth illustrates why brute-force enumeration of all valid generator commitment combinations quickly becomes intractable. To manage this complexity, we avoid exhaustive search by solving the unit commitment problem iteratively: each iteration only considers a manageable subset of decisions, and additional constraints are introduced in subsequent iterations to guide the solution away from unstable commitment patterns, such as cycling or oscillating generator decisions, i.e., repeatedly looping through statuses. The algorithm is explained in more detail in Section IV-A.

E. AC Optimal Power Flow with Load Shedding

The AC Optimal Power Flow (AC OPF) problem determines the optimal generation dispatch by solving the full nonlinear AC power flow equations while satisfying network constraints. Using generator commitment statuses from the unit commitment problem in (10) (solved with formulations such as DC power flow, first-order Taylor approximations, or CBLAs), we compute the dispatch for each online generator at each hour. The multi-period formulation minimizes the total cost across all hours while ensuring power balance and network feasibility at each time. If constraints prevent meeting full demand, load shedding is used as a last resort, with $L_{i,t}$ denoting the load shed at bus i and time t. The AC OPF with load shedding is formulated as follows:

$$\min \sum_{t \in \mathcal{T}} \left(\sum_{g \in \mathcal{G}} c_g(P_{g,t}) + \sum_{i \in \mathcal{B}} C^{\text{shed}}(L_{i,t}) \right) \tag{14a}$$

$$\text{s.t. } [\forall i \in \mathcal{B}, \forall t \in \mathcal{T}, \forall g \in \mathcal{G}, \forall (i,k) \in \mathcal{L}]$$

$$P_{i,t}^{\text{gen}} - P_{i,t}^{\text{load}} + L_{i,t} = \sum_{k \in \mathcal{B}} V_{i,t} V_{k,t} \Big(G_{ik} \cos \theta_{ik,t} + B_{ik} \sin \theta_{ik,t} \Big), \tag{14b}$$

$$Q_{i,t}^{\text{gen}} - Q_{i,t}^{\text{load}} + \beta_i L_{i,t} = \sum_{k \in \mathcal{B}} V_{i,t} V_{k,t} \Big(G_{ik} \sin \theta_{ik,t} - B_{ik} \cos \theta_{ik,t} \Big), \tag{14c}$$

$$P_{g,t}^{\min} u_{g,t} \leq P_{g,t} \leq P_{g,t}^{\max} u_{g,t}, \tag{14d}$$

$$Q_{g,t}^{\min} u_{g,t} \leq Q_{g,t} \leq Q_{g,t}^{\max} u_{g,t}, \tag{14e}$$

$$V_{i,t}^{\min} \leq V_{i,t} \leq V_{i,t}^{\max}, \tag{14f}$$

$$S_{ik,t} = \sqrt{P_{ik,t}^2 + Q_{ik,t}^2} \leq S_{ik}^{\max}, \tag{14g}$$

$$0 \leq L_{i,t} \leq P_{i,t}^{\text{load}}, \quad 0 \leq \beta_i L_{i,t} \leq Q_{i,t}^{\text{load}}, \tag{14h}$$

where $\beta_i = \tan \alpha_i$, given that $\cos \alpha_i$ represents the power factor associated with load i. The objective function in (14a) minimizes the total cost of generation over all time periods while penalizing load shedding using a function $C^{\text{shed}}(L_{i,t})$ to discourage demand curtailment unless necessary. The power balance constraints in (14b)–(14c) enforce the nonlinear AC power flow equations for active and reactive power at each bus and time period. The generator limits in (14d)–(14e) ensure that active and reactive power generation respects the unit commitment status $u_{g,t}$. The voltage limits in (14f) ensure that bus voltages remain within safe operating ranges. The thermal constraints in (14g) restrict apparent power flows on transmission lines to their rated capacities. Finally, the load shedding constraints in (14h) ensure that the curtailed demand remains non-negative and does not exceed the original load at any bus and time period. This formulation integrates the unit commitment results into AC OPF, optimizing the dispatch of committed generators while allowing for load shedding with constant power factors.

V. Numerical results

In this section, we conduct numerical experiments on several test cases to examine the behavior of CBLA, highlight the benefits of error function design, and demonstrate the effectiveness of CBLA in a UC problem.

The test cases used in the simulations are the IEEE 24-bus system and the IEEE 30-bus system, all of which are accessible in MATPOWER [23]. For approximations of voltage and current flow, we draw 500 samples by varying the power injections within a range of 70% to 130% of their nominal values. Both voltage and current flow values are reported in per unit (pu). We use the ℓ_1 norm as the loss function $\mathcal{L}(\cdot)$. The numerical simulation was conducted in MATLAB using Yalmip [24] and in Julia using the Optim package.

A. Conservative Bias Linear Approximations

We begin our numerical tests by examining the effects of changing the error function in (7) in our CBLA approach. As discussed in Section III-B, error functions are designed to balance conservativeness and accuracy. By testing various error functions, we aim to understand their impact on the number of violated samples and the accuracy of the approximated power flow equations.

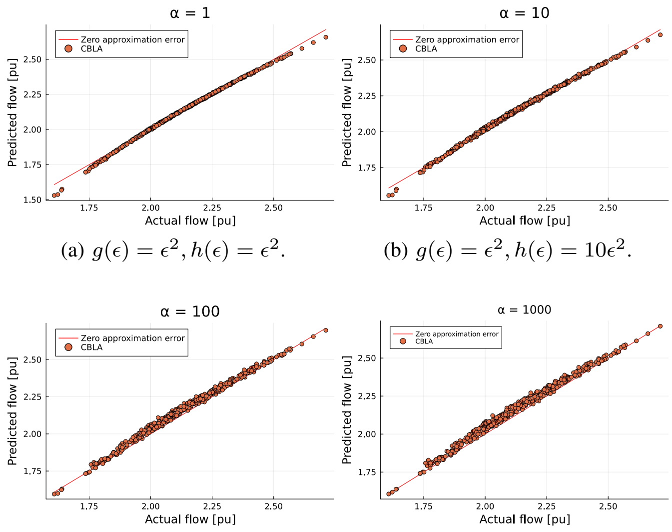

(a) $g(\epsilon) = \epsilon^2, h(\epsilon) = \epsilon^2$. (b) $g(\epsilon) = \epsilon^2, h(\epsilon) = 10\epsilon^2$.

(c) $g(\epsilon) = \epsilon^2, h(\epsilon) = 100\epsilon^2$. (d) $g(\epsilon) = \epsilon^2, h(\epsilon) = 1000\epsilon^2$.

Fig. 5. Plots of results when (a) $\alpha = 1$ (equivalent to the squared-ℓ_2 loss), (b) $\alpha = 10$, (c) $\alpha = 100$, and (d) $\alpha = 1000$ for current flow from bus 3 to bus 24 in IEEE 24-bus system. The red points represent overestimating CBLAs. The black line represents a zero approximation error.

In Fig. 5, we present the results of using the CBLA approach to intentionally overestimate the predicted current flow from bus 3 to bus 24 in IEEE 24-bus system using different quadratic error functions. The error functions used in this test are defined as $g(\epsilon) = \epsilon^2$ and $h(\epsilon) = \alpha\epsilon^2$, where α is a parameter that we vary across the test. Specifically, the parameter α modifies the bias in the CBLA formulation; a higher value of α increases the tendency toward conservativeness. We adjust α to take values of 1, 10, 100, and 1000. When $\alpha = 1$, the error functions are equivalent (i.e., $g(\epsilon) = h(\epsilon)$), implying no distinction in cost between violating and not violating conservativeness (i.e., the squared-ℓ_2 loss). In this scenario, most samples are well approximated, but some fall below the zero approximation error line, indicating a deviation from the overestimating objective.

Increasing α reduces the number of samples falling below the zero approximation error line, indicating better adherence to the overestimation goal. However, this improvement sacrifices overall accuracy. At $\alpha = 1000$, where most samples are intentionally overestimated, the accuracy tends to be lower compared to other scenarios. This trade-off highlights the importance of carefully selecting the value of α to achieve a suitable balance between overestimation and accuracy.

To gain further insight into the effects of varying α, we plot the relationship between the average error per sample of the approximated flow and the number of violated samples when varying the value of α in Fig. 6. In this test, we adjust α over a range from 1 to 10^4. The results reveal a clear trend: as α increases, the average error per sample also increases while the number of violated samples decreases significantly, demonstrating the trade-off between conservativeness and accuracy. This is due to the increased enforcement of conservativeness in the error function. Specifically, the average error per sample increases from 0.00869 when $\alpha = 1$ to 0.0455 when $\alpha = 10^4$,

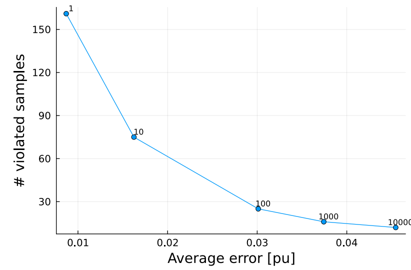

Fig. 6. Results showing the average error per sample in per unit (pu) and the number of violated samples due to overestimating CBLA of current flow from bus 3 to bus 24 in IEEE 24-bus system, as the value of α (labeled at each point) varies from 1 to 10^4.

while the number of violated samples decreases from 161 when $\alpha = 1$ to just 12 when $\alpha = 10^4$.

TABLE I
APPROXIMATED CURRENT FLOW ERRORS AND NUMBER OF VIOLATED SAMPLES AT REPRESENTATIVE BUSES IN IEEE 24-BUS SYSTEM

Line	Average errors/sample			# violated samples		
(From-to)	$\alpha = 1$	$\alpha = 10^2$	$\alpha = 10^4$	$\alpha = 1$	$\alpha = 10^2$	$\alpha = 10^4$
3-14	0.00869	0.03012	0.04551	161	25	12
6-10	0.00907	0.02274	0.03780	202	30	8
9-12	0.01621	0.04961	0.09397	180	29	6

The data in Table I illustrates the relationship between the number of violated samples and the average approximated current flow errors across different α values at different lines. These results align with the trend observed in Fig. 6, confirming that as α increases, the average error per sample increases while the number of violated samples decreases.

B. Application: Unit commitment

The comparison is conducted on the IEEE 30-bus test system, which has 6 generators. Voltage magnitude limits are set to 0.94 p.u. and 1.05 p.u. at all buses, and current magnitude limits are derived from the values in `mpc.branch(:,RATE_A)` in the MATPOWER case files. The cost of load shedding is $C^{\text{shed}}(L_{i,t}) = 500L_{i,t}$. We draw 1000 samples by varying power injections, both loads and generations, to cover possible load shedding and generation variation within a range of 70% to 130% of their nominal values. As shown in Table II, we report both the total cost, which includes load shedding penalties, and the generation-only cost, which excludes them to better isolate the impact of load shedding. Although the DC-based formulation often yields lower generation-only costs, it leads to much higher total costs due to frequent and severe load shedding. As illustrated in Fig. 7, the generator commitment schedules from CBLA differ from those of the DC and first-order Taylor methods, highlighting CBLA's ability to adapt commitment decisions based on a more accurate power flow approximation.

This difference is especially evident in hour 4, where the DC-based approach leads to 11.82% load shedding and a total cost of $20,417. In comparison, the first-order Taylor approximation reduces load shedding to 5.01%, with a much lower cost of $11,683. CBLA reduces load shedding even further to

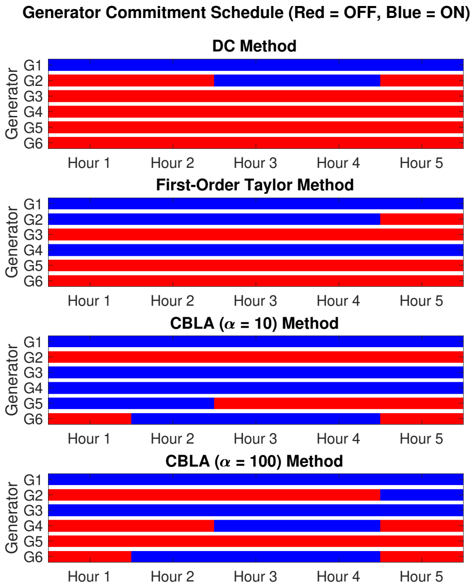

Fig. 7. Generator commitment schedules for the 30-bus system using three different power flow linearization methods: DC, first-order Taylor, and CBLA (when $\alpha = 10$ and 100). Each row block corresponds to a generator across five scheduling hours. Blue indicates the generator is ON, while red indicates it is OFF.

just 1.92%, while lowering the total cost to \$8,053.7—clearly demonstrating the value of its adaptive linearization.

While the DC and first-order Taylor methods rely on a single linearization of nonlinear power flows, CBLA builds a sample-based conservative approximation over a defined operating region, delivering significant improvements. Across all five hours, CBLA eliminates load shedding in four hours and limits it to minimal levels in the most challenging hour. CBLA consistently achieves the lowest total cost. For example, in hour 5, CBLA attains a lower total cost of \$3,958.8 compared to \$5,875 with the Taylor approximation and \$18,869 with the DC approximation.

The table also includes results for a more conservative CBLA variant with $\alpha = 100$. With $\alpha = 100$, the UC solution tends to avoid constraint violations. However, this added conservativeness comes at the cost of reduced accuracy in approximations. As a result, when the generation decisions from the UC problem are passed to the AC OPF, the resulting solution may still exhibit load shedding—particularly in Hour 5, where 0.93% of the demand remains unmet.

This trade-off underscores the need to balance conservativeness and approximation accuracy. CBLA's tunable parameter α allows us to adjust this balance to achieve the desired feasibility and flexibility. By tailoring the approximation to system conditions, CBLA helps reduce constraint violations and yields UC solutions that generally remain feasible under the nonlinear AC power flow model.

Moreover, the benefits of CBLA become more pronounced in larger systems or under tight feasibility margins. Unlike the first-order Taylor approximation, which is inherently local, CBLA is constructed to remain conservative across a sampled region of interest. This range-aware property improves

TABLE II
HOURLY COMPARISON ACROSS DIFFERENT APPROXIMATIONS

		H1	H2	H3	H4	H5
Load Demand (MW)		152.2	192.13	234.29	287.33	219.27
DC	Load Shedding (%)	0%	4.37%	2.57%	11.82%	15.23%
	Outputs (MW)					
	Gen 1	158.28	193.44	159.05	205.66	196.71
	Gen 2	0	0	80	61.62	0
	Gen 3 – Gen 6	0	0	0	0	0
	Total Cost (\$)	1818	6328	6090	20417	18869
	Gen-Only Cost (\$)	1817.6	2135.2	3076.1	3431.5	2167.3
First-Order Taylor	Load Shedding (%)	0%	0%	0.70%	5.01%	2.42%
	Outputs (MW)					
	Gen 1	52.84	85.27	134.71	202.56	189.72
	Gen 2	68.48	80	80	62.73	0
	Gen 3	0	0	0	0	0
	Gen 4	33.86	32.41	26.96	22.16	33.90
	Gen 5 – Gen 6	0	0	0	0	0
	Total Cost (\$)	3483	3682	4800	11683	5875
	Gen-Only Cost (\$)	3483.0	3682.1	3978.0	4480.5	3219.1
CBLA ($\alpha = 10$)	Load Shedding (%)	0%	0%	0%	1.92%	0%
	Outputs (MW)					
	Gen 1	58.14	58.32	99.31	152.81	127.40
	Gen 2	0	0	0	0	0
	Gen 3	26.96	27.47	45.73	46.77	50.00
	Gen 4	50.40	55.00	53.42	50.02	47.48
	Gen 5	18.73	24.61	0	0	0
	Gen 6	0	29.04	40	40	0
	Total Cost (\$)	4506.2	5660.4	4929.7	8053.7	3958.8
	Gen-Only Cost (\$)	4506.2	5660.4	4929.7	5299.5	3958.8
CBLA ($\alpha = 100$)	Load Shedding (%)	0%	0%	0%	1.92%	0.93%
	Outputs (MW)					
	Gen 1	110.53	110.45	99.31	152.81	100.66
	Gen 2	0	0	0	0	80.00
	Gen 3	45.01	45.40	45.73	46.77	42.51
	Gen 4	0	0	53.42	50.02	0
	Gen 5	0	0	0	0	0
	Gen 6	0	40.00	40.00	40.00	0
	Total Cost (\$)	2637.0	3799.1	4929.7	8053.7	4830.8
	Gen-Only Cost (\$)	2637.0	3799.1	4929.7	5299.5	3811.4

cost-efficiency in decision-making. Compared to traditional methods, CBLA provides a more adaptive solution framework that maintains the tractability of linear programming while reducing the gap between the models of linear and nonlinear power systems.

VI. CONCLUSION AND FUTURE WORK

This paper presents a conservative bias linear approximation (CBLA) approach for approximating the power flow equations, aiming to balance conservativeness and accuracy while preserving linearity. The numerical results highlight the potential advantages of using CBLA for power flow problems. Selecting suitable error functions enables an effective balance between conservativeness and accuracy. Additionally, the ability to choose different error functions allows CBLA to be tailored to specific systems and operational conditions. When applied to the unit commitment problem, the CBLA-based formulation consistently outperformed formulations based on DC power flow and first-order Taylor approximations, achieving lower overall operating costs in the subsequent evaluation of the AC optimal power flow.

In our future work, we aim to extend our current approach by developing additional conservative bias approximations through the use of piecewise linearizations. Moreover, we plan to apply our proposed approach to a broader range of power system planning and resilience tasks. This includes tackling complex bilevel problems, conducting capacity expansion planning studies, and extending the application of CBLA to unbalanced three-phase systems.

Acknowledgement

P. Buason thanks the Department of Mechatronics Engineering at Rajamangala University of Technology Phra Nakhon.

Appendix: First-Order Taylor Approximation of Voltage and Current Constraints

Suppose the power injections $\boldsymbol{P}$ and $\boldsymbol{Q}$ deviate from their nominal values $\boldsymbol{P}^{\text{nom}}$ and $\boldsymbol{Q}^{\text{nom}}$. Let $\mathcal{B}^{\text{PQ}}$ denote the set of PQ buses, $\widetilde{V}_{i,t}$ denote the first-order Taylor approximation of the voltage magnitude at bus i and time t, and let the abbreviation "nom" indicate that a quantity is evaluated at the nominal operating point, which is computed separately for each hour based on the corresponding loads. For each $i \in \mathcal{B}^{\text{PQ}}$, the first-order Taylor approximation of the voltage magnitude is:

$$\widetilde{V}_{i,t} = V_i^{\text{nom}} + \left.\frac{\partial V_i}{\partial \boldsymbol{P}}\right|_{\text{nom}} \cdot (\boldsymbol{P}_t - \boldsymbol{P}^{\text{nom}}) + \left.\frac{\partial V_i}{\partial \boldsymbol{Q}}\right|_{\text{nom}} \cdot (\boldsymbol{Q}_t - \boldsymbol{Q}^{\text{nom}}), \tag{15}$$

where the partial derivatives $\frac{\partial V_i}{\partial \boldsymbol{P}}$ and $\frac{\partial V_i}{\partial \boldsymbol{Q}}$ are evaluated at the nominal operating point using the inverse of the power flow Jacobian. For non-PQ buses, the voltage magnitude is fixed at its nominal value:

$$\widetilde{V}_{i,t} = V_i^{\text{nom}}, \quad \forall i \notin \mathcal{B}^{\text{PQ}}. \tag{16}$$

To model current flow limits, we approximate the real part of the power flow on each transmission line $(i,k) \in \mathcal{L}$ using the difference in bus voltage magnitudes from (16):

$$\Re(S_{ik,t}) \approx |Y_{ik}| \cdot (\widetilde{V}_{i,t} - \widetilde{V}_{k,t}), \tag{17}$$

where $\Re(\,\cdot\,)$ denotes the real part of a complex quantity and $|Y_{ik}|$ is the magnitude of the admittance between buses i and k. We then enforce the following absolute value inequality to approximate current magnitude limits:

$$-I_{ik}^{\max} \le |Y_{ik}| \cdot (\widetilde{V}_{i,t} - \widetilde{V}_{k,t}) \le I_{ik}^{\max},\ \forall (i,k) \in \mathcal{L},\ \forall t \in \mathcal{T}. \tag{18}$$

To allow controlled violations of these approximations similar to (11)–(12), slack variables may be added as needed in the optimization formulation.

References

[1] R. Gupta, P. Buason, and D. K. Molzahn, "Fairness-aware photovoltaic generation limits for voltage regulation in power distribution networks using conservative linear approximations," in *8th Texas Power and Energy Conference (TPEC)*, Feb. 2024.

[2] A. D. Owen Aquino, S. Talkington, and D. K. Molzahn, "Managing vehicle charging during emergencies via conservative distribution system modeling," in *8th Texas Power and Energy Conference (TPEC)*, Feb. 2024.

[3] N. Bhusal, M. Abdelmalak, M. Kamruzzaman, and M. Benidris, "Power system resilience: Current practices, challenges, and future directions," *IEEE Access*, vol. 8, pp. 18 064–18 086, 2020.

[4] A. Castillo, C. Laird, C. A. Silva-Monroy, J.-P. Watson, and R. P. O'Neill, "The unit commitment problem with AC optimal power flow constraints," *IEEE Trans. Power Syst.*, vol. 31, no. 6, pp. 4853–4866, 2016.

[5] L. P. I. Sampath, M. Hotzt, H. B. Gooi, and W. Utschick, "Unit commitment with AC power flow constraints for a hybrid transmission grid," in *20th Power Systems Computation Conference (PSCC)*, 2018.

[6] P. Buason, S. Misra, S. Talkington, and D. K. Molzahn, "A data-driven sensor placement approach for detecting voltage violations in distribution systems," *Electric Power Systems Research*, vol. 232, p. 110387, 2024.

[7] S. Wogrin, S. Pineda, and D. A. Tejada-Arango, *Applications of Bilevel Optimization in Energy and Electricity Markets*. Cham: Springer International Publishing, 2020, pp. 139–168.

[8] B. Stott, J. Jardim, and O. Alsaç, "DC power flow revisited," *IEEE Trans. Power Syst.*, vol. 24, no. 3, pp. 1290–1300, Aug. 2009.

[9] M. E. Baran and F. F. Wu, "Optimal capacitor placement on radial distribution systems," *IEEE Trans. Power Del.*, vol. 4, no. 1, pp. 725–734, Jan. 1989.

[10] D. K. Molzahn and I. A. Hiskens, "A survey of relaxations and approximations of the power flow equations," *Foundations and Trends in Electric Energy Systems*, vol. 4, no. 1-2, pp. 1–221, Feb. 2019.

[11] S. Misra, D. K. Molzahn, and K. Dvijotham, "Optimal adaptive linearizations of the AC power flow equations," in *20th Power Systems Computation Conference (PSCC)*, June 2018.

[12] P. Buason, S. Misra, and D. K. Molzahn, "A sample-based approach for computing conservative linear power flow approximations," *Electric Power Systems Research*, vol. 212, p. 108579, 2022, presented at the *22nd Power Systems Computation Conference (PSCC 2022)*.

[13] P. Buason, S. Misra, J.-P. Watson, and D. K. Molzahn, "Adaptive power flow approximations with second-order sensitivity insights," *IEEE Trans. Power Syst.*, vol. 40, no. 3, pp. 2648–2660, 2025.

[14] J. Chen and L. A. Roald, "A data-driven linearization approach to analyze the three-phase unbalance in active distribution systems," *Electric Power Systems Research*, vol. 211, p. 108573, 2022, presented at the *22nd Power Systems Computation Conference (PSCC 2022)*.

[15] M. Jia and G. Hug, "Overview of data-driven power flow linearization," in *IEEE Belgrade PowerTech*, 2023.

[16] M. Jia, G. Hug, N. Zhang, Z. Wang, and Y. Wang, "Tutorial on data-driven power flow linearization–Part I: Challenges and training algorithms," preprint available at https://doi.org/10.3929/ethz-b-000606654, 2023.

[17] ——, "Tutorial on data-driven power flow linearization–Part II: Supportive techniques and experiments," preprint available at https://doi.org/10.3929/ethz-b-000606656, 2023.

[18] P. Buason, S. Misra, and D. K. Molzahn, "Sample-based conservative bias linear power flow approximations," in *2024 IEEE/IAS Industrial and Commercial Power System Asia (I&CPS Asia)*, 2024, pp. 1–6.

[19] N. Padhy, "Unit commitment–A bibliographical survey," *IEEE Trans. Power Syst.*, vol. 19, no. 2, pp. 1196–1205, 2004.

[20] "Optim.jl - An optimization framework for Julia," https://julianlsolvers.github.io/Optim.jl/stable/, accessed: 2024-04-14.

[21] H. Happ, "Optimal power dispatch – A comprehensive survey," *IEEE Trans. Power Apparatus and Syst.*, vol. 96, no. 3, pp. 841–854, 1977.

[22] K. Van den Bergh, E. Delarue, and W. D'haeseleer, "DC power flow in unit commitment models," KU Leuven, TME Working Paper, Tech. Rep. WP EN2014-02, 2014.

[23] R. D. Zimmerman, C. E. Murillo-Sánchez, and R. J. Thomas, "MATPOWER: Steady-state operations, planning, and analysis tools for power systems research and education," *IEEE Trans. Power Syst.*, vol. 26, no. 1, pp. 12–19, Feb. 2011.

[24] J. Löfberg, "YALMIP: A toolbox for modeling and optimization in MATLAB," in *IEEE International Symposium on Computer Aided Control Systems Design (CACSD)*, September 2004, pp. 284–289.